



Manuscript received 25 September 2019 Revised manuscript received 17 December 2019 Manuscript accepted 26 December 2019

© 2020 Geological Society of America. For permission to copy, contact editing@geosociety.org

A critical magma chamber size for volcanic eruptions

Meredith Townsend¹ and Christian Huber²

¹Department of Earth Sciences, University of Oregon, 100 Cascade Hall, Eugene, Oregon 97403, USA ²Department of Earth, Environmental, and Planetary Sciences, Brown University, 324 Brook Street, Providence, Rhode Island 02906, USA

ABSTRACT

We present a model for a coupled magma chamber-dike system to investigate the conditions required to initiate volcanic eruptions and to determine what controls the size of eruptions. The model combines the mechanics of dike propagation with internal chamber dynamics including crystallization, volatile exsolution, and the elastic response of the magma and surrounding crust to pressure changes within the chamber. We find three regimes for dike growth and eruptions: (1) below a critical magma chamber size, eruptions are suppressed because chamber pressure drops to lithostatic before a dike reaches the surface; (2) at an intermediate chamber size, the erupted volume is less than the dike volume ("dike-limited" eruption regime); and (3) above a certain chamber size, dikes can easily reach the surface and the erupted volume follows a classic scaling law, which depends on the attributes of the magma chamber ("chamber-limited" eruption regime). The critical chamber volume for an eruption ranges from ~0.01 km³ to 10 km³ depending on the water content in the magma, depth of the chamber, and initial overpressure. This implies that the first eruptions at a volcano likely are preceded by a protracted history of magma chamber growth at depth, and that the crust above the magma chamber may have trapped several intrusions or "failed eruptions." Model results can be combined with field observations of erupted volume, pressure, and crystal and volatile content to provide tighter constraints on parameters such as the eruptible chamber size.

INTRODUCTION

Determining what allows magma to reach the surface and what controls the amount and rate of volcanic output has profound implications for the assessment of volcanic hazards. Eruption rates, styles, and sizes are influenced by overpressure in crustal magma chambers as well as the dynamics of ascent through dikes or conduits that connect magma chambers to the surface (e.g., Cashman, 2004; Gonnermann and Manga, 2007; Moran et al., 2011; Wong et al., 2017). Huppert and Woods (2002) presented an idealized model for effusive eruptions fed by chamber overpressure; assuming a fixed conduit geometry, they found a scaling law for the total volume of erupted material $(V_{\rm er})$:

$$V_{\rm er} = V_{\rm ch} \beta \Delta P,$$
 (1)

where $V_{\rm ch}$ is chamber volume, β is the effective compressibility of the system (host rocks and magma), and ΔP is the total pressure drop in the chamber during the eruption. Within this framework, magmatic volatiles may

significantly influence $V_{\rm er}$ by increasing β by more than an order of magnitude (Huppert and Woods, 2002). This model points to the importance of internal magma chamber processes on the erupted volume, like volatile exsolution concurrent with the eruption. However, it neglects some aspects of magma dynamics (e.g., crystallization caused by exsolution during decompression) as well as the processes involved in the propagation of a dike and transport of magma to the surface.

The scaling law of Huppert and Woods (2002) has been supported by subsequent models that take into account conduit physics (e.g. Anderson and Segall, 2011; Melnik and Sparks, 2005). Crystallization and volatile exsolution in the conduit affect the mass flux and behavior of an eruption, but the final amount of erupted material remains a function of magma chamber conditions and is well approximated by the scaling law. Comparison of predicted and observed erupted volumes lends further support for the scaling law, e.g. Mount St. Helens (Anderson and Segall, 2011; Mastin et al., 2008), Campi

Flegrei, Laguna del Maule, Aso, and Santorini (Townsend et al., 2019).

One aspect missing from existing magma chamber models is dike propagation. For many volcanoes, eruptions initiate through fissures fed by dikes, so eruptions depend on the mechanics of the dike and whether it can reach the surface. Coupled dike-chamber models such as those of Segall et al. (2001), Rivalta and Segall (2008), Rivalta (2010), and Buck et al. (2006) were developed for diking events at basaltic rift zones like Kilauea (Hawaii, USA) and Iceland. While some of these models address the influence of volatiles on magma compressibility, the full coupling between pressure change during growth of an intrusion and phase changes in the magma are typically neglected, and none of these models have been adapted to understand more silicic, water-rich arc volcanoes. In this paper, we present a new dike-chamber model that considers both internal magma chamber dynamics and propagation of dikes, with the goal of understanding how these processes affect the occurrence and size of eruptions at silicic volcanoes.

MODEL

The model we present combines the magma chamber lumped model of Degruyter and Huber (2014) with the dike-chamber model of Segall et al. (2001). The chamber is a spherical volume of eruptible magma containing silicate melt, crystals, and dissolved and exsolved water. The crystal volume fraction in the chamber evolves according to a melting curve parameterized for dacite after Huber et al. (2009), and the water solubility follows the parameterization of Dufek and Bergantz (2005) and Zhang (1999). The chamber resides in a colder viscoelastic crust. but because we focus on single eruptions that occur on short time scales, the crust is essentially elastic and the thermodynamic state of the chamber is affected primarily by magma withdrawal leading to heat loss and decompression. Recharge rates are generally much slower than

CITATION: Townsend, M., and Huber, C., 2020, A critical magma chamber size for volcanic eruptions: Geology, v. 48, p. G47045.1

, https://doi.org/10.1130/

eruption rates, so recharge is neglected here. The change in mass in the chamber with time (dM_c/dt) is balanced by mass flux into the dike, $q_{\rm dike}$, which we assume is proportional to the pressure difference between the chamber, P_c , and dike, P_d :

$$\frac{dM_{\rm c}}{dt} = -q_{\rm dike} = \gamma (P_{\rm c} - P_{\rm d}). \tag{2}$$

The constant γ represents the "conductivity" between the chamber and dike and depends on the geometry of their connection. For simplicity, the results presented here are calculated with $\gamma=1$ kg/Pa·s; we show in the GSA Data Repository¹ that this value only modestly affects the time-integrated results.

Conservation of water mass, $M_{\rm w}$, and enthalpy, H, leads to:

$$\frac{dM_{\rm w}}{dt} = -q_{\rm dike} (\chi_{\rm d} + \chi_{\rm e}), \tag{3}$$

$$\frac{dH}{dt} = -cTq_{\text{dike}} - Q_{\text{cond}},\tag{4}$$

where χ_d and χ_e are dissolved and exsolved water mass fractions in the magma, respectively, c is heat capacity, T is temperature, and Q_{cond} is the rate of heat flow from the chamber into the surrounding crust. The first term in Equation 4 represents heat advected out of the chamber by flow into the dike, and the second term represents heat conducted from the chamber into the crust (effectively negligible on the time scale of most eruptions).

The dike is a vertically oriented half-ellipsoid, with half-length a and half-height b. Initially, the dike dimensions are small compared to the chamber depth d, with $a_0 = 0.02d$ and $b_0 = a_0/2$. Dike growth is governed by the pressure gradients available to drive magma with viscosity η to flow laterally and vertically through the fracture (Segall et al., 2001):

$$\frac{da}{dt} = \frac{\delta^2}{3\eta} \left(\frac{\Delta P_{\rm d}}{a} \right),\tag{5}$$

$$\frac{db}{dt} = \frac{\delta^2}{3\eta} \left(\frac{\Delta P_{\rm d}}{b} - \Delta \rho g \right), \text{ in which } \Delta P_{\rm d} > \Delta \rho g b,$$

otherwise
$$\frac{db}{dt} = 0$$
, (6)

where δ is the maximum aperture of the dike, ΔP_d is the overpressure at the dike inlet, and $\Delta \rho$ is the density difference between the bulk magma and crust, and g is gravity. In this work, magma density evolves as a function of crystal and volatile fraction, but is always positively buoyant. The maximum aperture of the dike, δ , is governed by elastic deformation of the host rock:

$$\delta = \frac{2b(1-v)\Delta P_{\rm d}}{\mathsf{u}E(k)},\tag{7}$$

where μ and v are the elastic stiffness and Poisson's ratio of the crust, respectively, and E(k) is the elliptic integral of the second kind with modulus k (Segall et al., 2001).

If the dike reaches the surface (b = d), we account for the eruptive flux q_{erupt} when conserving mass in the dike (M_{d}) :

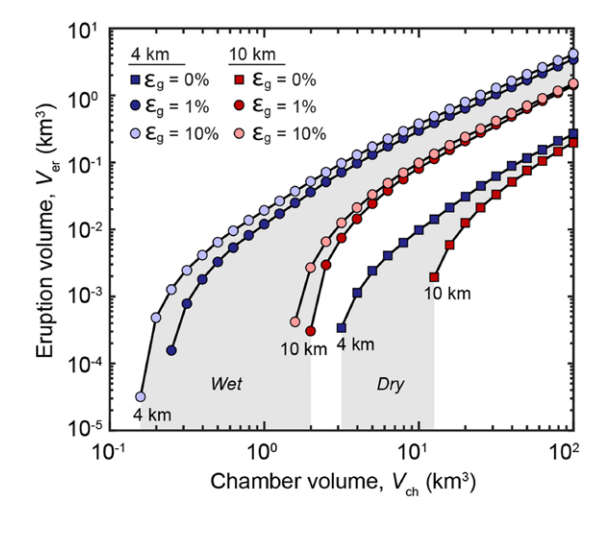
$$\frac{dM_d}{dt} = q_{\text{dike}} - q_{\text{erupt}},\tag{8}$$

where q_{erupt} depends on the vertical pressure gradient, the dike aperture, and the length of the

eruptive fissure, which we set here to be 0.5a (we expand on $q_{\rm erupt}$ in the Data Repository, and show that changing this fraction does not impact the results). We do not consider erosion of the fissure or the development of more cylindrical shapes, which may impact the evolution of the eruptive flux (e.g., Wadge, 1981; Aravena et al., 2018).

Initially, the dike (P_d) and chamber (P_c) pressure $P_{d}(0) = P_{c}(0) = P_{lit} + P_{crit}$, where P_{lit} is lithostatic pressure and $P_{\rm crit}$ is the magma overpressure required to initiate a dike. P_{crit} depends on factors such as the strength of the crust, the prevalence of preexisting fractures, and the shape of the chamber and whether stress is concentrated along the chamber walls (Gregg et al., 2012; Jellinek and DePaolo, 2003; Rubin, 1995). To account for these possible variations, we explore a range of $P_{\rm crit}$ from 10 to 50 MPa. As the dike grows, P_d drops, facilitating flow from the chamber to the dike. The model terminates when $P_{\rm c} = P_{\rm d}$ (there is no longer a pressure gradient), or when there is no longer enough overpressure at the dike inlet to prevent freezing, i.e., when $P_{\rm d} < P_{\rm lit} + 2$ MPa (Rubin, 1995). This criterion is a simplified way to approximate effects of heat loss in the dike, because we do not explicitly model thermodynamic processes in the dike. Magma density and gas fraction evolve in the chamber, which sets inflow conditions for the dike, but once the magma enters the dike its properties are fixed. By neglecting vesiculation in the dike, we may underestimate the total volume erupted, so these results should be considered minimum bounds. In addition, the magma viscosity η is constant, and the thermal effects of viscosity are not considered. Thus in our results (see the Data Repository), and in similar models (Segall et al., 2001; Anderson and Segall, 2011), η only affects the time evolution of an eruption and not the total erupted volume.

Equations 2–6 and 8, expanded on in the Data Repository, compose a set of six ordinary differential equations for P_c , P_d , T, exsolved wa-



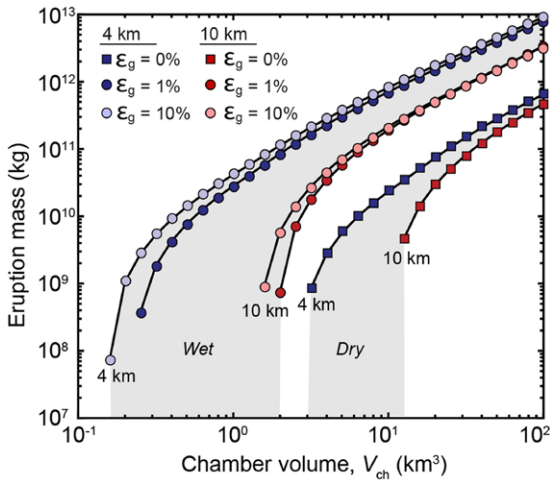


Figure 1. Erupted magma volumes (left) and erupted mass (right) as a function of chamber volume for different initial volume fractions of exsolved volatiles (ε_a) and different chamber depths. Blue dots represent 4 km depth, red dots represent 10 km depth. Gray shaded areas correspond to saturated cases (initial exsolved volatile fraction is >0; "wet") or undersaturated cases (exsolved volatile fraction = 0 and no exsolution takes place during the eruption; "dry"). Magma overpressure required to initiate dike, P_{crit} = 10 MPa.

¹GSA Data Repository item 2020120, expanded governing equations, an analysis of the effects of magma viscosity, dike-chamber conductivity, and fissure length, and a derivation of the effective magma compressibility, is available online at http://www.geosociety.org/datarepository/2020/, or on request from editing@geosociety.org.

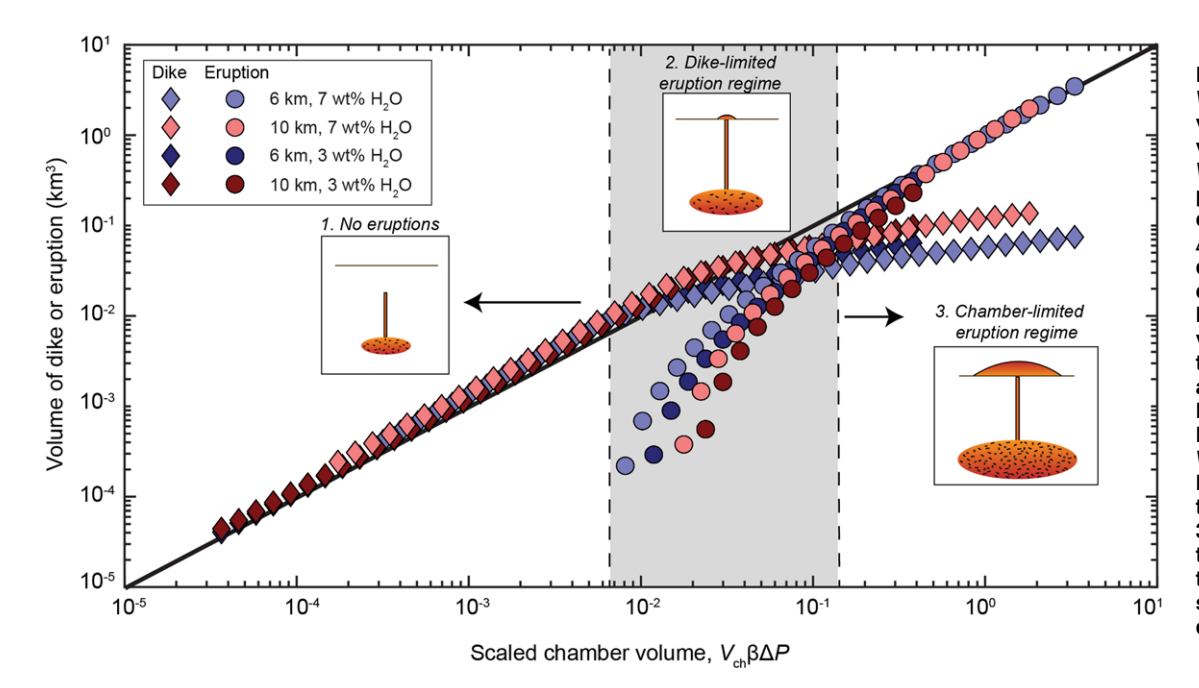


Figure 2. Eruption volume, $V_{\rm er}$ (circles), and dike volume (diamonds) versus chamber volume, V_{ch}, scaled by magma compressibility, β, and initial chamber overpressure. ΔP . Colors correspond to different depths and water contents. In regime 1 (lefthand side), $V_{er} = 0$, and volume of dikes follows the scaling of Huppert and Woods (2002; black line). In regime 2 ("dikelimited eruption regime"), $V_{er} = 0$ but is significantly less than that indicated by the scaling law. In regime 3 ("chamber-limited eruption regime"), V_{er} follows the scaling law and is significantly greater than dike volume.

ter content $\varepsilon_{\rm g}$, and dike height b and length a. We solve the equations in MATLAB software using the ode15s solver. Results were validated by comparing simplified cases with the original model results of Degruyter and Huber (2014) and Segall et al. (2001). Eruption volumes $V_{\rm er}$ are calculated by integrating $q_{\rm crupt}$ over time, and the dike volumes are calculated by $V_{\rm d} = \frac{\pi}{3} ab\delta$. Because we do not model conduit physics like bubble growth, $V_{\rm er}$ is akin to a dense-rock equivalent (DRE).

RESULTS

The final volume of magma erupted, $V_{\rm er}$, is primarily a function of the chamber volume $V_{\rm ch}$. Figure 1 shows $V_{\rm er}$ versus $V_{\rm ch}$ for simulations run at different depths (4–10 km) and initial exsolved water contents ($\varepsilon_{\rm g}=0\%$ [and undersaturated during dike growth], 1%, and 10% volume fractions). When $V_{\rm ch}$ is less than a critical volume, $V_{\rm crit}$, eruptions do not occur because pressure $P_{\rm c}$ or $P_{\rm d}$ drops below a critical threshold (either $P_{\rm c}=P_{\rm d}$ or $P_{\rm d}< P_{\rm lit}+2$ MPa) before dikes reach the surface. Once $V_{\rm ch}>V_{\rm crit}$, $V_{\rm er}$ increases nonlinearly with $V_{\rm ch}$ before increasing linearly at greater $V_{\rm ch}$ (Fig. 1).

Eruption volume $V_{\rm er}$ is sensitive to the presence of an exsolved volatile phase. While there is little difference in $V_{\rm er}$ between magmas with $\varepsilon_{\rm g}=1\%$ and $\varepsilon_{\rm g}=10\%$, magma chambers with $\varepsilon_{\rm g}=1\%$ can produce eruptions more than two orders of magnitude greater than chambers containing no exsolved volatiles (Fig. 1). The jump in $V_{\rm er}$ between dry and wet magmas occurs because the exsolution of a low-density volatile phase in wet magmas maintains greater pressure in the chamber, effectively increasing the compressibility β by more than an order of magnitude (see the Data Repository for the derivation

of β). Because volatiles exsolve more readily at lower pressures, we also see greater $V_{\rm er}$ at shallower depths (Fig. 1). However, this is also partly due to dikes being initially closer to the surface and thus consuming less of the withdrawn magma to reach it.

Figure 2 compares $V_{\rm cr}$ to the scaling relationship by Huppert and Woods (2002) (Equation 1). Three regimes are apparent: below a critical chamber volume ($V_{\rm ch} < V_{\rm crit}$), no eruptions occur, but the volume of dikes $V_{\rm d}$ follows the scaling law (Equation 1). At intermediate $V_{\rm ch}$, eruptions occur, but the majority of magma leaving a chamber is stored in the dike. Beyond this regime ($V_{\rm ch} >> V_{\rm crit}$), $V_{\rm er}$ is closely approximated by the scaling law $V_{\rm ch}\beta\Delta P$. In this regime, $V_{\rm d} << V_{\rm er}$ and dikes do not pose a significant limit on eruptions. Moreover, the collapse of calculated $V_{\rm er}$ for different amounts of water with respect to

the scaled chamber volume $V_{ch}\beta\Delta P$ confirms that the primary influence of volatiles is to change β (Fig. 2).

The main effect of the dike is to limit the amount of magma that erupts. Only when $V_{ch} >$ $V_{\rm crit}$ can eruptions occur. $V_{\rm crit}$ can vary between ~0.01 km3 and 10 km3 depending on chamber depth, water content, and initial overpressure $P_{\rm crit}$ (Fig. 3). In general, $V_{\rm crit}$ is greater for deeper chambers, in part because of the requirement for dikes to reach the surface and in part because of the increased solubility of volatiles. In Figure 3, we see that $V_{\rm crit}$ in the driest and wettest systems (3 and 7 wt% H₂O) is only weakly sensitive to depth. In the dry case, magma never reaches volatile saturation to form a compressible fluid phase; the depth dependence of $V_{\rm crit}$ is solely a reflection of the requirement for dikes to reach the surface. Similarly, in the wettest case, magma always con-

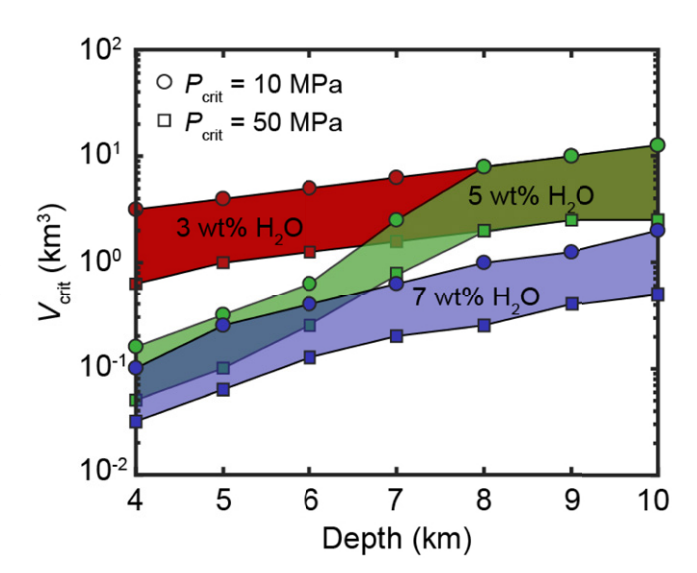


Figure 3. Critical chamber volume, $V_{\rm crit}$, to initiate eruptions at the surface as function of chamber depth (x-axis), water content (red = 3 wt%, green = 5 wt%, blue = 7 wt%), and initial chamber overpressure, $P_{\rm crit}$ (circles = 10 MPa, squares = 50 MPa).

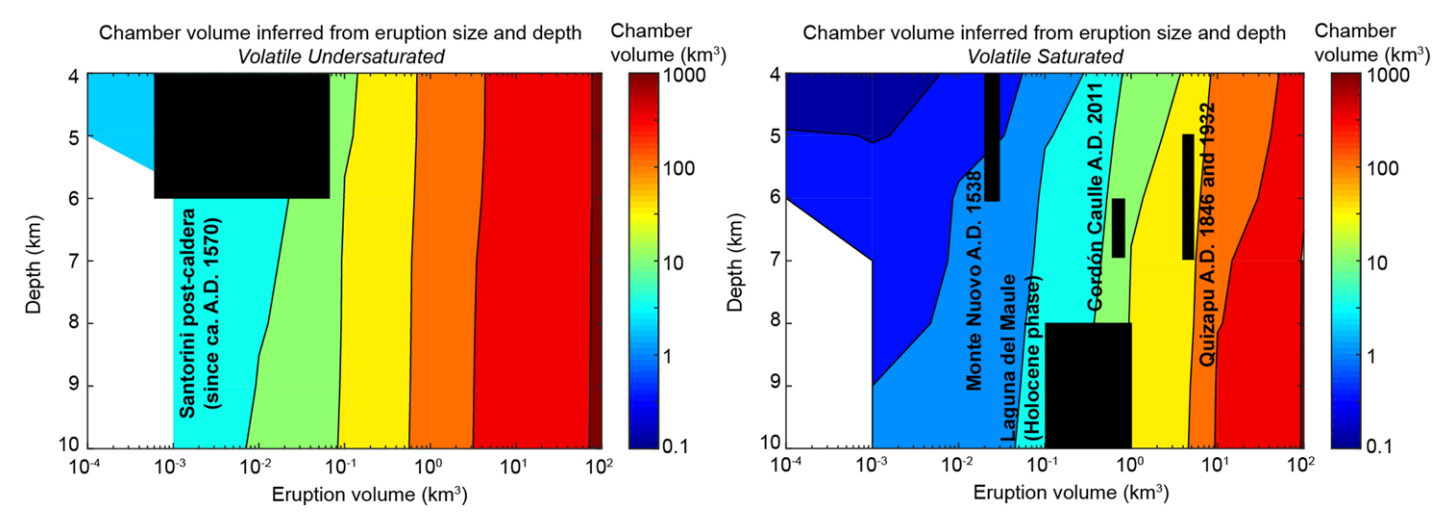


Figure 4. Chamber volumes (colored values) as function of eruption size (x-axis), depth (y-axis), and volatile saturation state (left, under-saturated; right, saturated). Black boxes are examples of inferred chamber volume from post-caldera Santorini (Greece) (Parks et al., 2012; Degruyter et al., 2016); Monte Nuovo eruption of Campi Flegrei (Italy) (Di Vito et al., 1987; Forni et al., 2018); 2011 eruption of Cordón Caulle (Chile) (Singer et al., 2008; Jay et al., 2014); Laguna del Maule (Chile) throughout the Holocene (Hildreth et al., 2010; Singer et al., 2014; Andersen et al., 2017); and the twin eruptions at Quizapu (Chile) (Hildreth and Drake, 1992; Ruprecht et al., 2012). White space covers parameters for which no eruptions are predicted to occur (chamber volume [V_{ch}] smaller than critical chamber volume to initiate eruption at surface [V_{crit}]).

tains an exsolved fluid phase regardless of depth; $V_{\rm crit}$ in these cases is also controlled by dike propagation. For intermediate water content (5 wt%), we see a greater spread of $V_{\rm crit}$ with depth, reflecting the combined influence of dike propagation and pressure-dependent water solubility. Finally, $V_{\rm crit}$ also depends on the initial chamber overpressure $P_{\rm crit}$ (Fig. 3). For a given water content and depth, increasing $P_{\rm crit}$ from 10 to 50 MPa reduces $V_{\rm crit}$ by almost one order of magnitude (Fig. 3). This is in agreement with Segall et al. (2001), who found that the ratio of magmastatic head to initial overpressure controlled the ability of dikes to reach the surface, with greater overpressures leading to dikes that erupt more easily.

DISCUSSION AND CONCLUSIONS

The existence of a critical chamber size needed to produce eruptions raises questions about how volcanoes develop. For many silicic systems, subvolcanic magma chambers are thought to grow at depths of ~7-10 km or ~2 kbar (Huber et al., 2019); prior to significant in situ crystallization and fractionation, magmas may be relatively dry (<5 wt% H₂O). For these conditions, $V_{\rm crit}$ is between ~1 and 10 km³ (Fig. 3), already the scale inferred for plumbing systems at many long-lived volcanoes; e.g., present-day estimates at Campi Flegrei (Italy) and Santorini (Greece) (Degruyter et al., 2016; Forni et al., 2018). For a magma recharge rate of ~0.001 km³/yr, growth of the chamber to these sizes may take 1-10 k.y. (Townsend et al., 2019), implying that subvolcanic reservoirs may spend long periods of time brewing in the crust before expressing themselves at the surface.

The model results relating $V_{\rm er}$, $V_{\rm ch}$, depth, and volatile saturation allow the use of geo-

logic and petrologic data (P-T-X-volatiles and DRE volume) to infer the size of the underlying chamber that fed a particular eruption. In Figure 4, we compile examples from several well-studied volcanic episodes such as the Holocene phase at Laguna del Maule (Chile) and the post-caldera eruptions at Santorini. Based on the average size of eruptions at Laguna del Maule, ~0.1-1 km³ (Hildreth et al., 2010; Singer et al., 2014), and the likely water-saturated conditions of the erupted products (Andersen et al., 2017), $V_{\rm ch}$ inferred from the model is between ~5 and 20 km³ (Fig. 4), in reasonable agreement with estimates from a gravity survey by Miller et al. (2017). Although the eruptions of post-caldera Santorini are smaller on average, at ~0.001-0.02 km3 (Parks et al., 2012), the inferred V_{ch} of ~5–10 km³ is on a similar scale (Fig. 4), reflecting the dry post-caldera conditions in the chamber at Santorini compared to Laguna del Maule (Degruyter et al., 2016).

Although we focus on eruption potential and eruption size, the dike-chamber model presented here can be applied more generally to understand the influence of internal magma chamber processes on dike geometries and propagation rates. Over long time scales as magma reservoirs cool and evolve chemically, magma compressibility, density, and viscosity change, which in turn affect the direction and rates of dike propagation. In that way, dike characteristics may be a reflection of how a magma chamber has evolved over time; field observations of eroded dikes could provide insight on the magmatic history, or intrusion events at active volcanoes could be used to infer present-day magma and chamber properties.

ACKNOWLEDGMENTS

Funding for this work was provided in part by the U.S. National Science Foundation grant EAR-1760004 to Huber and Townsend. All data from the volcanic systems used to produce Figure 4 come from published literature cited in the references. MATLAB code for the model will be made available upon request. We thank Paul Segall and two anonymous reviewers for constructive reviews that improved the manuscript.

REFERENCES CITED

Andersen, N.L., Singer, B.S., Jicha, B.R., Beard, B.L., Johnson, C.M., and Licciardi, J.M., 2017, Pleistocene to Holocene growth of a large upper crustal rhyolitic magma reservoir beneath the active Laguna del Maule volcanic field, central Chile: Journal of Petrology, v. 58, p. 85–114, https://doi .org/10.1093/petrology/egx006.

Anderson, K., and Segall, P., 2011, Physics-based models of ground deformation and extrusion rate at effusively erupting volcanoes: Journal of Geophysical Research, v. 116, B07204, https://doi.org/10.1029/2010JB007939.

Aravena, A., Cioni, R., de' Michieli Vitturi, M., Pistolesi, M., Ripepe, M., and Neri, A., 2018, Evolution of conduit geometry and eruptive parameters during effusive events: Geophysical Research Letters, v. 45, p. 7471–7480, https://doi.org/10.1029/2018GL077806.

Buck, W.R., Einarsson, P., and Brandsdottir, B., 2006, Tectonic stress and magma chamber size as controls on dike propagation: Constraints from the 1975–1984 Krafla rifting episode: Journal of Geophysical Research, v. 111, B12404, https://doi.org/10.1029/2005JB003879.

Cashman, K.V., 2004, Volatile controls on magma ascent and eruption, *in* Sparks, R.S.J., and Hawkesworth, C.J., eds., The State of the Planet: Frontiers and Challenges in Geophysics: American Geophysical Union Geophysical Monograph 150, p. 109–124, https://doi.org/10.1029/150GM10.

Degruyter, W., and Huber, C., 2014, A model for eruption frequency of upper crustal silicic magma chambers: Earth and Planetary Science Letters, v. 403, p. 117–130, https://doi.org/10.1016/j.epsl.2014.06.047.

- Degruyter, W., Huber, C., Bachmann, O., Cooper, K.M., and Kent, A.J.R., 2016, Magma reservoir response to transient recharge events: The case of Santorini volcano (Greece): Geology, v. 44, p. 23–26, https://doi.org/10.1130/G37333.1.
- Di Vito, M., Lirer, L., Mastrolorenzo, G., and Rolandi, G., 1987, The 1538 Monte Nuovo eruption (Campi Flegrei, Italy): Bulletin of Volcanology, v. 49, p. 608–615, https://doi.org/10.1007/BF01079966.
- Dufek, J., and Bergantz, G.W., 2005, Transient twodimensional dynamics in the upper conduit of a rhyolitic eruption: A comparison of closure models for the granular stress: Journal of Volcanology and Geothermal Research, v. 143, p. 113–132, https://doi.org/10.1016/j.jvolgeores.2004.09.013.
- Forni, F., Degruyter, W., Bachmann, O., De Astis, G., and Mollo, S., 2018, Long-term magmatic evolution reveals the beginning of a new caldera cycle at Campi Flegrei: Science Advances, v. 4, eaat9401, https://doi.org/10.1126/sciadv.aat9401.
- Gonnermann, H.M., and Manga, M., 2007, The fluid mechanics inside a volcano: Annual Review of Fluid Mechanics, v. 39, p. 321–356, https://doi.org/10.1146/annurev.fluid.39.050905.110207.
- Gregg, P.M., de Silva, S.L., Grosfils, E.B., and Parmigiani, J.P., 2012, Catastrophic caldera-forming eruptions: Thermomechanics and implications for eruption triggering and maximum caldera dimensions on Earth: Journal of Volcanology and Geothermal Research, v. 241, p. 1–12, https://doi.org/10.1016/j.jvolgeores.2012.06.009.
- Hildreth, W., and Drake, R.E., 1992, Volcan Quizapu, Chilean Andes: Bulletin of Volcanology, v. 54, p. 93–125, https://doi.org/10.1007/BF00278002.
- Hildreth, W., Godoy, E., Fierstein, J., and Singer, B., 2010, Laguna del Maule volcanic field: Eruptive history of a Quaternary basalt-to-rhyolite distributed volcanic field on the Andean rangecrest in central Chile: Servicio Nacional de Geología y Minería–Chile Boletin 63, 142 p.
- Huber, C., Bachmann, O., and Manga, M., 2009, Homogenization processes in silicic magma chambers by stirring and mushification (latent heat buffering): Earth and Planetary Science Letters, v. 283, p. 38–47, https://doi.org/10.1016/ j.epsl.2009.03.029.
- Huber, C., Townsend, M., Degruyter, W., and Bachmann, O., 2019, Optimal depth of subvolcanic magma chamber growth controlled by volatiles and crust rheology: Nature Geoscience, v. 12, p. 762–768, https://doi.org/10.1038/s41561-019-0415-6.

- Huppert, H.E., and Woods, A.W., 2002, The role of volatiles in magma chamber dynamics: Nature, v. 420, p. 493–495, https://doi.org/10.1038/ nature01211.
- Jay, J., Costa, F., Pritchard, M., Lara, L., Singer, B., and Herrin, J., 2014, Locating magma reservoirs using InSAR and petrology before and during the 2011–2012 Cordón Caulle silicic eruption: Earth and Planetary Science Letters, v. 395, p. 254–266, https://doi.org/10.1016/j.epsl.2014.03.046.
- Jellinek, A.M., and DePaolo, D.J., 2003, A model for the origin of large silicic magma chambers: Precursors of caldera-forming eruptions: Bulletin of Volcanology, v. 65, p. 363–381, https://doi .org/10.1007/s00445-003-0277-y.
- Mastin, L.G., Roeloffs, E., Beeler, N.M., and Quick, J.E., 2008, Constraints on the size, overpressure, and volatile content of the Mount St. Helens magma system from geodetic and dome growth measurements during the 2004–2006+ eruption, in Sherrod, D.R., et al., eds., A Volcano Rekindled: The Renewed Eruption of Mount St. Helens, 2004–2006: U.S. Geological Survey Professional Paper 1750, p. 461–488, https://doi.org/10.3133/ pp175022.
- Melnik, O., and Sparks, R.S.J., 2005, Controls on conduit magma flow dynamics during lava dome building eruptions: Journal of Geophysical Research, v. 110, B02209, https://doi.org/10.1029/2004JB003183.
- Miller, C.A., Williams-Jones, G., Fournier, D., and Witter, J., 2017, 3D gravity inversion and thermodynamic modelling reveal properties of shallow silicic magma reservoir beneath Laguna del Maule, Chile: Earth and Planetary Science Letters, v. 459, p. 14–27, https://doi.org/10.1016/ j.epsl.2016.11.007.
- Moran, S.C., Newhall, C., and Roman, D.C., 2011, Failed magmatic eruptions: Late-stage cessation of magma ascent: Bulletin of Volcanology, v. 73, p. 115–122, https://doi.org/10.1007/s00445-010-0044.x
- Parks, M.M., et al., 2012, Evolution of Santorini Volcano dominated by episodic and rapid fluxes of melt from depth: Nature Geoscience, v. 5, p. 749–754, https://doi.org/10.1038/ngeo1562.
- Rivalta, E., 2010, Evidence that coupling to magma chambers controls the volume history and velocity of laterally propagating intrusions: Journal of Geophysical Research, v. 115, B07203, https://doi.org/10.1029/2009JB006922.
- Rivalta, E., and Segall, P., 2008, Magma compressibility and the missing source for some dike

- intrusions: Geophysical Research Letters, v. 35, L04306, https://doi.org/10.1029/2007GL032521.
- Rubin, A.M., 1995, Getting granite dikes out of the source region: Journal of Geophysical Research, v. 100, p. 5911–5929, https://doi .org/10.1029/94JB02942.
- Ruprecht, P., Bergantz, G.W., Cooper, K.M., and Hildreth, W., 2012, The crustal magma storage system of Volcán Quizapu, Chile, and the effects of magma mixing on magma diversity: Journal of Petrology, v. 53, p. 801–840, https://doi.org/10.1093/petrology/egs002.
- Segall, P., Cervelli, P., Owen, S., Lisowski, M., and Miklius, A., 2001, Constraints on dike propagation from continuous GPS measurements: Journal of Geophysical Research, v. 106, p. 19,301– 19,317, https://doi.org/10.1029/2001JB000229.
- Singer, B.S., Jicha, B.R., Harper, M.A., Naranjo, J.A., Lara, L.E., and Moreno-Roa, H., 2008, Eruptive history, geochronology, and magmatic evolution of the Puyehue-Cordón Caulle volcanic complex, Chile: Geological Society of America Bulletin, v. 120, p. 599–618, https://doi.org/10.1130/ B26276.1.
- Singer, B.S., et al., 2014, Dynamics of a large, restless, rhyolitic magma system at Laguna del Maule, southern Andes, Chile: GSA Today, v. 24, no. 12, p. 4–10, https://doi.org/10.1130/GSATG216A.1.
- Townsend, M., Huber, C., Degruyter, W., and Bachmann, O., 2019, Magma chamber growth during intercaldera periods: Insights from thermo-mechanical modeling with applications to Laguna del Maule, Campi Flegrei, Santorini, and Aso: Geochemistry Geophysics Geosystems, v. 20, p. 1574–1591, https://doi.org/10.1029/2018GC008103.
- Wadge, G., 1981, The variation of magma discharge during basaltic eruptions: Journal of Volcanology and Geothermal Research, v. 11, p. 139–168, https://doi.org/10.1016/0377-0273(81)90020-2.
- Wong, Y.-Q., Segall, P., Bradley, A., and Anderson, K., 2017, Constraining the magmatic system at Mount St. Helens (2004–2008) using Bayesian inversion with physics-based models including gas escape and crystallization: Journal of Geophysical Research: Solid Earth, v. 122, p. 7789– 7812, https://doi.org/10.1002/2017JB014343.
- Zhang, Y.X., 1999, Exsolution enthalpy of water from silicate liquids: Journal of Volcanology and Geothermal Research, v. 88, p. 201–207, https://doi .org/10.1016/S0377-0273(98)00115-2.

Printed in USA